

Investigation of Asphaltene Association with Vapor Pressure Osmometry and Interfacial Tension Measurements

Harvey W. Yarranton,* Hussein Alboudwarej, and Rajesh Jakher

Department of Chemical and Petroleum Engineering, University of Calgary, 2500 Univeristy Drive NW, Calgary, Alberta, Canada T2N 1N4

Molar masses of both *n*-pentane-extracted and *n*-heptane-extracted Athabasca asphaltenes were measured in toluene or 1,2-dichlorobenzene with a vapor pressure osmometer (VPO). The initial asphaltene molar mass, at concentrations below 0.5 kg/m³, is ≈ 1800 g/mol. The asphaltene molar mass is found to increase with asphaltene concentration until a limiting value is reached at a concentration between 10 and 20 kg/m³. The limiting value ranges from 4000 to 10 000 g/mol and depends on the solvent, temperature, and asphaltene fraction. The results suggest that asphaltenes form aggregates of 2–6 molecules in aromatic solvents. Interfacial tensions of asphaltenes in toluene or 1,2-dichlorobenzene versus water were measured for asphaltene concentrations from 0.3 to 100 kg/m³ using a drop volume tensiometer. The interfacial tension decreases linearly with concentration, indicating that no micelles are formed. Hence, the aggregation observed with VPO does *not* appear to be micellization. Similar results are obtained for Cold Lake asphaltenes.

Introduction

Asphaltene precipitation and the nature of asphaltenes in solution have been studied for the past 50 years and are still being debated. Part of the challenge is that asphaltenes are a solubility class and not a pure component; here, they are defined as the part of a crude oil that is soluble in toluene and insoluble in *n*-pentane or *n*-heptane. Hence, they consist of many thousands of chemical species and their composition is not well defined. In addition, they appear to interact with each other and other oil constituents in a complex manner. It has been proposed that they exist as free molecules in a nonideal solution,¹ as aggregates of asphaltenes and resins,² as colloidal particles,³ or as reverse micelles.⁴ The various proposed structures have led to two different types of models for asphaltene precipitation: the thermodynamic¹ and colloidal models.⁵ The thermodynamic model presumes that the asphaltenes are part of a nonideal mixture and that their behavior is governed by continuum thermodynamics. The colloidal model presumes that the asphaltenes are colloidal particles surrounded by adsorbed resins. The resins are assumed to partition between the asphaltene particles and the solvent. If sufficient resins desorb, the asphaltenes aggregate and precipitate. The thermodynamic model predicts that asphaltene precipitation is reversible while the colloidal model predicts irreversible precipitation. In fact, there appears to be a hysteresis in asphaltene precipitation.^{6,7} Hence, while the colloidal model is more generally accepted, it is still not clear which, if either, model is correct. Therefore, it is necessary to identify the structure of asphaltenes in crude oils.

The asphaltene colloidal model arose from X-ray crystallography data, demonstrating that solid asphaltenes consisted of stacked aromatic sheets held together

by π - π bonding. It was proposed that small stacks of asphaltenes were dispersed in a crude oil by resins.³ The colloidal model is supported by small-angle neutron scattering and small-angle X-ray scattering measurements that detected spherical, or possibly disk-shaped, particles with diameters of ≈ 8 nm dispersed both in crude oils and in asphaltene-toluene mixtures.^{8–11}

Other work suggests that asphaltenes form reverse micelles rather than stacks of molecules. Micelles and reverse micelles are surfactant aggregates. *Micelles* are aggregates in which the hydrophobic parts of the surfactants are concentrated in the center of the aggregate while the hydrophilic parts reside on the surface. Micelles occur in the aqueous phase where the hydrophobic part of the surfactant is aligned away from the water and the hydrophilic part resides near the water. *Reverse micelles* occur in the oil phase and the surfactant alignment is the opposite from that of a micelle; that is, the hydrophilic parts of the surfactants are concentrated within the aggregate. Micelles are expected to form above a threshold concentration, the critical micelle concentration (cmc). Reverse micelles have not been investigated in detail and it is not known if they exhibit a cmc. However, from calorimetry experiments, an apparent dissociation energy was observed upon dilution of asphaltene-toluene-heptane mixtures below a critical concentration.¹² Furthermore, several investigators have observed a change in oil-water interfacial tension versus asphaltene concentration consistent with reverse micelle formation.^{13–15}

One tool that can be used to shed light on asphaltene association is vapor pressure osmometry (VPO). With VPO, the molar mass of asphaltenes can be measured as a function of concentration in any single-component solvent. Hence, asphaltene association in a solvent can be quantified by measuring the change in molar mass. In fact, previous VPO studies have demonstrated that different molar masses are observed at different asphaltene concentrations, temperatures, and solvents.^{16,17} In this paper, asphaltene molar mass and solvent-

* To whom correspondence should be addressed. Phone: (403) 220-6529. Fax: (403) 282-3945. E-mail: hyarrant@ucalgary.ca.

Table 1. Athabasca and Cold Lake Bitumen Composition

bitumen fraction	present work		literature	
	Athabasca	Cold Lake	Athabasca	Cold Lake
saturates (wt %)	16.3	19.4	17.3 ¹⁸	20.7 ¹⁸
aromatics (wt %)	39.8	38.1	39.7 ¹⁸	39.7 ¹⁸
resins (wt %)	26.4	26.7	25.8 ¹⁸	24.8 ¹⁸
C5-asphaltenes (wt %)	17.5	15.8	17.3 ¹⁸	15.3 ¹⁸
toluene insolubles (wt % of C5-asphaltenes)	6.5			
C7-asphaltene (wt %)	13.4	11.3	14.5 ¹⁹	
toluene insolubles (wt % of C7-asphaltenes)	7.8	2.3	6.3 ¹⁹	

water interfacial tensions are reported for a range of asphaltene concentrations in toluene and 1,2-dichlorobenzene. The relationship between interfacial tension and asphaltene association is examined and the reverse micelle model is tested. In addition, the interpretation of VPO data for asphaltenes is discussed.

Experimental Method

Materials. Asphaltenes were extracted from Athabasca and Cold Lake bitumens. Athabasca bitumen is an oil-sands bitumen and a coker feed sample was supplied by Syncrude Canada Ltd. Coker feed bitumen has been treated to remove most of the sand and water and is ready for upgrading. The Cold Lake bitumen is recovered from an underground reservoir by cyclic steam injection. It was supplied by Imperial Oil Ltd. of Canada and has also been treated to remove most of the sand and water. A SARA analysis of each bitumen sample is given in Table 1.

Asphaltenes were extracted from the bitumen using either *n*-heptane or *n*-pentane as the precipitant. The procedure was the same for each precipitant. For example, *n*-heptane was added to the bitumen at a 40:1 volume ratio of *n*-heptane:bitumen. The mixture was sonicated for 45 min and left to settle overnight. The supernatant liquid was removed and the remaining precipitate was further diluted with *n*-heptane at a 4:1 heptane:bitumen volume ratio. The final mixture was filtered through Whatman #2 filter paper (8 μm) and washed with *n*-heptane until no discoloration was observed in the washings. Note that this washing step proved crucial for obtaining accurate molar mass measurements because small amounts of low molar mass impurities can significantly affect the number-average molar mass. For example, the measured molar mass of "unwashed" asphaltenes was as much as 50% lower than that of "washed" asphaltenes. The asphaltenes were then dried at 70 °C under a nitrogen blanket until there was no further change in mass. Asphaltenes extracted with *n*-heptane will be referred to as the "C7-asphaltenes" and those extracted with *n*-pentane as the "C5-asphaltenes". The respective asphaltene contents of the Athabasca and Cold Lake bitumens are reported in Table 1.

With some crude oils, non-asphaltenic solids (consisting of clay, sand, and some adsorbed hydrocarbons²⁰) coprecipitate with the asphaltenes. To remove the solids, the asphaltenes were dissolved in toluene, typically at a concentration of 10 g of asphaltene/L of toluene. The mixture was centrifuged at 900 g for 5 min. The supernatant was removed and dried in a rotary evaporator at 70 °C under vacuum. The fractions of the C5- and C7-asphaltenes that did not dissolve in toluene are

reported in Table 1. In all cases, the nondissolving fraction is <8 wt % of the asphaltenes. Note that centrifuging will not remove ultrafine solids that make up ≈2% of the asphaltenes.²⁰ The non-asphaltene solids do not appear to influence interfacial tension,¹⁹ but their effect on vapor pressure osmometry measurements is unknown. However, it is not likely that the small amount of remaining solids will cause significant error because solid-phase material is not expected to interact appreciably with the solvent and influence vapor pressure. All the vapor pressure osmometry and interfacial tension measurements were conducted with asphaltenes that were treated to remove the non-asphaltene solids.

Reagent-grade *n*-heptane and *n*-pentane were obtained from Phillips Chemical Co., toluene (99.9% purity) was obtained from VWR, and 1,2-dichlorobenzene (99% HPLC grade) was obtained from Sigma Aldrich Co. Distilled water, light mineral oil, and octacosane were also obtained from Sigma Aldrich. Sucrose octacetate was supplied by Jupiter Instrument Co.

Vapor Pressure Osmometry. Vapor pressure osmometry is based on the difference in vapor pressure caused by the addition of a small amount of solute to a pure solvent. In the vapor pressure osmometer, a droplet of pure solvent and a droplet of solvent-solute are placed on separate thermistors surrounded by pure solvent vapor. The difference in vapor pressure between the two droplets results in a difference in temperature at each thermistor. The temperature difference causes a voltage difference, which is related to the molar mass of the solute as follows,¹⁸

$$\frac{\Delta E}{C_2} = K \left(\frac{1}{M_2} + A_1 C_2 + A_2 C_2^2 + \dots \right) \quad (1)$$

where ΔE is the voltage difference between the thermistors, C_2 is the concentration of the solute, K is the calibration constant, and A_i represents the coefficients. The higher order terms arise from nonideal solution behavior. To calibrate the instrument, solutes that form nearly ideal mixtures with the solvent at low concentrations are chosen. Most of the higher order terms become negligible, and eq 1 reduces to

$$\frac{\Delta E}{C_2} = \frac{K}{M_2} + K A_1 C_2 \quad (2)$$

Because the solute molar mass is known, the calibration constant can be determined from the intercept of a plot of $\Delta E/C_2$ versus C_2 .

Once the instrument is calibrated, the voltage differences for solutions of asphaltenes and pure solvent can be measured. However, it is not known at what conditions asphaltenes form ideal or nonideal mixtures. In benzene and toluene, asphaltene VPO molar mass does not appear to change with concentration,^{16,19} possibly indicating that an ideal solution has formed. In other more polar solvents, such as 1,2-dichlorobenzene, the measured molar mass appears to change linearly with concentration. Most authors assume that the correct asphaltene molar mass can be found from the intercept of a plot of $\Delta E/C_A$ versus C_A , where C_A is the asphaltene concentration.^{16,18,21}

Asphaltene molar mass was measured with a Jupiter Model 833 vapor pressure osmometer. Sucrose octacetate (679 g/mol) was used to calibrate the instrument and octacosane (395 g/mol) was used to check the

Table 2. Interfacial Tension of Organic Solvents versus Distilled Water

solvent	interfacial tension (mN/m)	
	present work	literature
<i>n</i> -heptane	49.2	50.1 ²²
benzene	34.7	34.0 ²²
toluene	35.5	35.8 ²²

calibration. The measured molar mass of octacosane was found to be within 2% of the correct value. There was considerable variation in the voltage at any given condition probably because of slight local temperature fluctuations, and therefore at least three runs over the same range of concentrations were performed.

Interfacial Tension. Interfacial tensions between hydrocarbon mixtures and distilled water were measured with a Kruss Model DVT10 drop volume tensiometer. In a drop volume tensiometer, one liquid is flowed through a thin-walled capillary into a second liquid and a series of drops form at the tip of the capillary. Each drop detaches when the buoyancy force acting on the drop equals the tension holding it to the capillary tip. At this point, the interfacial tension is given by

$$\sigma = \frac{V_{\text{drop}} g \Delta \rho}{\pi d} = \frac{Q t g \Delta \rho}{\pi d} \quad (3)$$

where σ is the interfacial tension, V_{drop} is the drop volume at detachment, Q is the volumetric flow rate of the drop-forming liquid, g is the gravitational acceleration, $\Delta \rho$ is the density difference between the two liquids, d is the diameter of the capillary tip, and t is the time from initiation to detachment for each drop. Note that the effect of the asphaltenes on the density of the asphaltene–solvent mixture must be accounted for, especially at high asphaltene concentrations. An asphaltene density of 1200 kg/m³¹⁹ was used to make the correction. This density was measured indirectly from asphaltene–toluene mixtures, which appear to form ideal solutions up to at least 10 kg/m³ asphaltene concentration.

The flow rate is controlled with a Harvard Apparatus Model 44 syringe pump accurate to within $\pm 1\%$. When each droplet detaches, it passes a photodiode and detector and the time is recorded. The difference in the time at which each drop passes the detector is the time to detachment. Interfacial tensions can generally be found to within ± 0.1 mN/m for drop volumes between 0.25 and 1.0 cm³. Interfacial tensions were measured for a number of pure solvents versus water and are compared with literature values in Table 2. The agreement is within 2% in all cases.

However, the instrument has some limitations. At flow rates above 2.0 cm³/h, inertial forces become significant and eq 3 is no longer valid. At high viscosity, elasticity affects the adherence force, also invalidating eq 3. Another factor affecting the accuracy of the measured interfacial tension is neck formation between the drop and the capillary tip. If a neck forms, the circumference around which the adherence force acts is smaller than the capillary tip and eq 3 does not apply. The use of thin-walled capillary tips reduces this source of error. Campanelli and Wang²³ found that the DVT10 drop volume tensiometer gives accurate results when the less dense component forms the drop. Necking did occur when the denser fluid formed the drop and

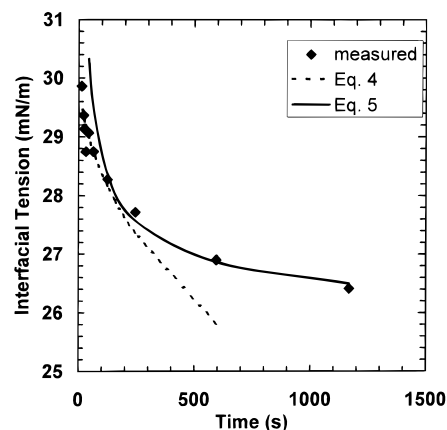


Figure 1. Dynamic interfacial tension of 15 kg/m³ Athabasca C7-asphaltenes in toluene versus water.

interfacial tension exceeded 18 mN/m. Significant *absolute* errors in interfacial tension were observed at these conditions. However, Campanelli and Wang found that in many cases the error could be corrected by using an effective diameter in eq 3 and that the effective diameter did not change with the flow rate. Hence, the surfactant diffusion rate and change in interfacial tension upon surfactant addition could still be determined accurately.

The drop volume tensiometer measures dynamic interfacial tension. Interfacial tension depends on the composition at the interface, which in turn depends on the relative adsorption of the different components in the liquids. A finite time is required for the components to diffuse to the interface. Typically, the time for a drop to detach from the capillary tip in a drop volume tensiometer is insufficient for the interface to reach equilibrium. The higher the flow rate, the shorter the detachment time and the further the interfacial tension is from equilibrium. Equilibrium interfacial tensions can be found by fitting a surfactant adsorption equation to interfacial tensions measured at different detachment times (flow rates). For example, the interfacial tension of 15 kg/m³ of Athabasca C7-asphaltenes in toluene versus water is given in Figure 1. The early-time data were fitted with the following equation²⁴ appropriate for limited diffusion times,

$$\sigma = \sigma_s - 2RTC_A' \sqrt{\frac{3Dt}{7\pi}} \quad (4)$$

and the late-time data were fitted with the approximation for long diffusion times,²⁵

$$\sigma = \sigma_{\text{eq}} + \frac{RT\Gamma^2}{C_A'} \left(\frac{7\pi}{12Dt} \right)^{1/2} \quad (5)$$

where C_A' is the asphaltene molar concentration (mmol/m³), σ_{eq} is the equilibrium interfacial tension (N/m), σ_s is the pure solvent interfacial tension (N/m), R is the universal gas constant (J/(mol K)), T is the temperature (K), Γ is the asphaltene surface coverage (mol/m²), and D is the diffusivity (m²/s). The fitted equilibrium interfacial tension is 25.6 mN/m. This value is very close to the interfacial tension of 25.0 mN/m measured with a deNuoy ring tensiometer for the same system after 2 h of contact time.¹⁹

It would require a large number of experiments to obtain equilibrium interfacial tensions for the range of

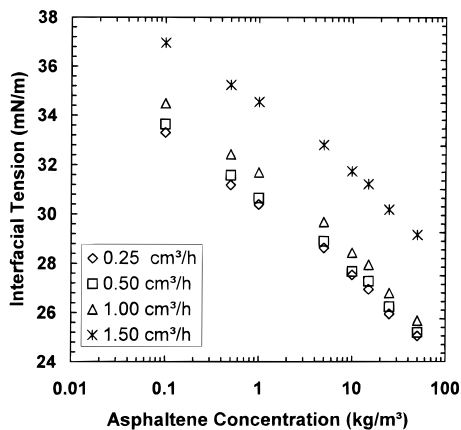


Figure 2. Effect of flow rate on measured interfacial tension for Athabasca C7-asphaltenes in toluene versus water.

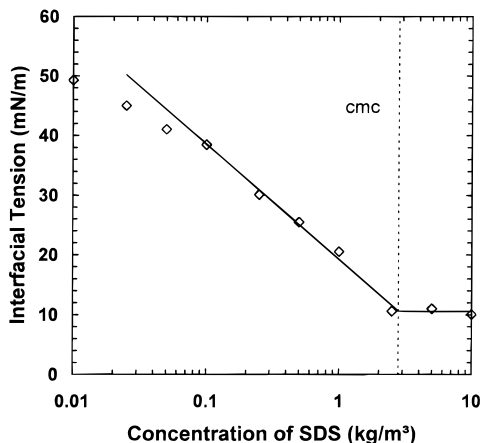


Figure 3. Interfacial tension of SDS in water versus light mineral oil at 50 °C at a flow rate of 1.0 cm³/h.

conditions investigated in this paper. As will be discussed later, our interest is in the slope of interfacial tension versus the log of asphaltene concentration. Fortunately, equilibrium interfacial tensions are not required to obtain the slope. Interfacial tensions of Athabasca C7-asphaltenes in toluene versus water were measured at different flow rates (detachment times) and are plotted in Figure 2. The slopes decrease slightly from -1.42 to -1.31 mN/m as the flow rate decreases from 1.5 to 0.25 cm³/h. However, the change is $<8.5\%$. Now, a flow rate of 0.25 cm³/h corresponds to a detachment time of 245 s. At this time, interfacial tension is approaching equilibrium as shown in Figure 1. Hence, experiments conducted at a single flow rate <1.5 cm³/h are expected to give the desired slopes to within 10% of the slopes that would be reached at equilibrium.

Note that, when required, the temperature was controlled by immersion of the capillary tube and its surrounding liquid-filled chamber in a water bath. Flow rates of 0.25 and 1.0 cm³/h were employed at temperatures of 25 and 50 °C, respectively. The higher flow rate was used at 50 °C to minimize exposure of the photodiode to hot water.

Results and Discussion

The relationship between interfacial tension and surfactant concentration for a typical surfactant system, sodium dodecyl sulfonate (SDS) in water versus light mineral oil, is given in Figure 3. A linear decrease in surface tension with an increase in surfactant concen-

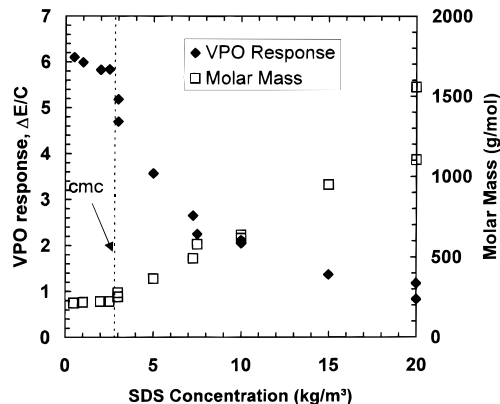


Figure 4. VPO measurements of SDS in water at 50 °C.

Table 3. Properties of Sodium Dodecyl Sulfonate Micelles

	present work (50 °C)	literature ²⁶ (25 °C)
cmc from IFT (kg/m ³)	2.8 ± 0.5	2.3
cmc from VPO (kg/m ³)	2.8 ± 0.5	
monomer molar mass (g/mol)	220	288
monomers per micelle	36	80

tration occurs when the interface is saturated with surfactant at equilibrium with the bulk phase. However, the surface tension becomes constant above the critical micelle concentration. When micelles form, every additional surfactant molecule becomes part of a non-surface-active micelle. The concentration of free surfactant is then constant and consequently so is the interfacial tension.

The number-average molar mass for such a system is expected to equal the monomer molar mass below the cmc and to be an average of the monomer and micelle molar mass above the cmc. At sufficiently high concentrations, the number of micelles will far exceed the number of monomers and the average molar mass will equal the micelle molar mass.

The molar mass for the SDS/water system was measured with VPO and is shown in Figure 4. On the left axis, the results are presented as $\Delta E/C_A$ versus SDS concentration. The value of $\Delta E/C_A$ is constant until the cmc concentration is reached. Therefore, a truncated form of eq 2 was used to calculate the apparent molar mass:

$$M = \frac{KC_A}{\Delta E} \quad (6)$$

The apparent molar mass is plotted on the right axis of Figure 4. The results of the IFT and VPO measurements are compared with literature values in Table 3.

These results confirm that a combination of interfacial tensions and vapor pressure osmometry experiments can be used to verify the presence of micelles and give an estimate of their size. The monomer molar mass is 24% lower than the correct molar mass, reflecting the potential error in VPO measurements if only a few data points are collected. In this case, the error may arise from the calibration or from a blank run that is part of the VPO procedure. However, the point was not pursued because the qualitative results were sufficient to demonstrate micellization.

Asphaltene Molar Mass Measurements. A plot of $\Delta E/C_A$ versus asphaltene concentration for Athabasca C5-asphaltenes in toluene is given in Figure 5. The

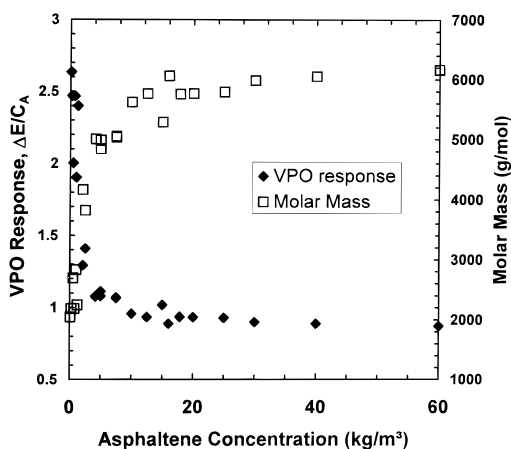


Figure 5. VPO measurements of Athabasca C5-asphaltenes in toluene at 50 °C.

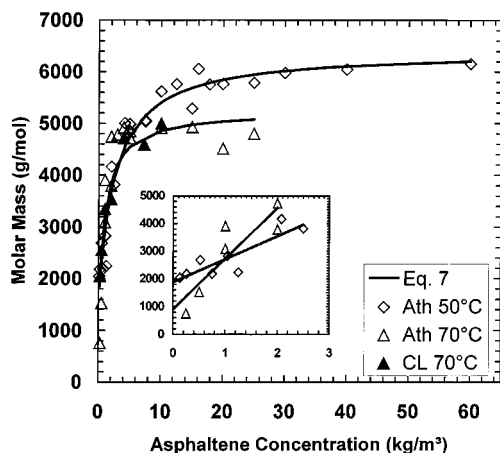


Figure 6. VPO molar mass of Athabasca (Ath) and Cold Lake (CL) C5-asphaltenes in toluene. The insert shows the low-concentration Athabasca data on an expanded scale with the linear extrapolation to infinite dilution.

apparent molar mass from eq 6 is shown on the same plot. There is a linear decrease in $\Delta E/C_A$ (or increase in apparent molar mass) as the asphaltene concentration increases, but a limiting value is reached at a concentration of $\approx 20 \text{ kg/m}^3$. The change in $\Delta E/C_A$ could be caused by nonideal solution behavior. However, with nonideal behavior, departures from ideality are expected to be minimal at low concentrations and significant at high concentrations. The VPO measurements show the opposite behavior. Hence, it is more likely that the change in VPO response reflects a change in the asphaltene molar mass; that is, some form of association occurs.

The VPO apparent molar mass of Athabasca C5- and C7-asphaltenes in toluene are shown in Figures 6 and 7, respectively, and in 1,2-dichlorobenzene in Figures 8 and 9, respectively. In all cases, the asphaltenes show an increase in molar mass as the asphaltene concentration increases but reach a limiting molar mass. If the shape of the plot of molar mass versus asphaltene concentration is a result of asphaltene association and not nonideal solution behavior, then the standard technique for determining molar mass will give misleading results. Recall that usually the measured molar mass is linearly extrapolated to zero concentration to find the "correct" molar mass. Consider Figure 6. On one hand, if the molar masses of the C5-asphaltenes were measured in toluene at 50 °C from concentrations

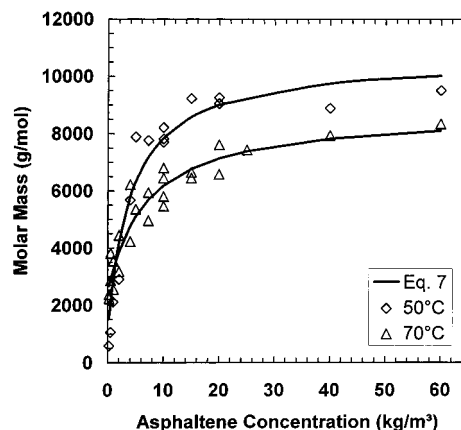


Figure 7. VPO molar mass of Athabasca C7-asphaltenes in toluene.

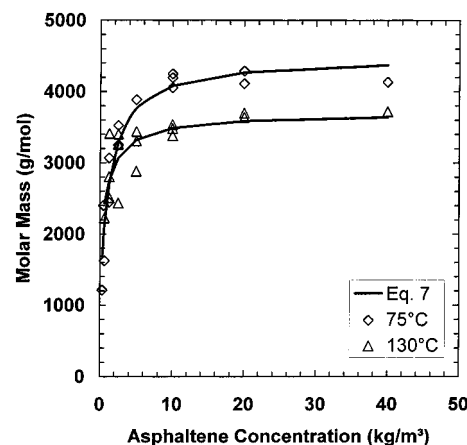


Figure 8. VPO molar mass of Athabasca C5-asphaltenes in 1,2-dichlorobenzene.

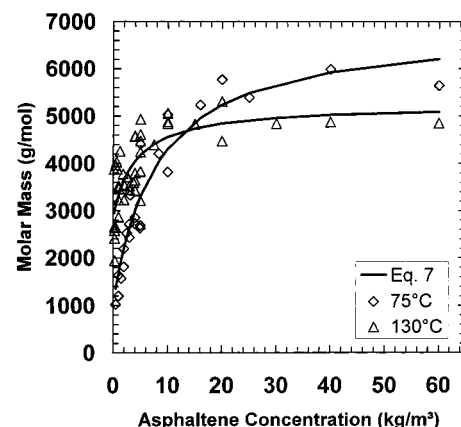


Figure 9. VPO molar mass of Athabasca C7-asphaltenes in 1,2-dichlorobenzene.

between 20 and 50 kg/m^3 ($\approx 2\text{--}5 \text{ wt } \%$), then a molar mass of $\approx 5500 \text{ g/mol}$ would be estimated from the linear extrapolation. On the other hand, an extrapolation over concentrations from 1 to 5 kg/m^3 would give a molar mass of $\approx 1500 \text{ g/mol}$. In fact, both concentration ranges have been used by different researchers.^{16–19,21} Some of the variations in reported asphaltene molar masses may be due to the different concentrations used in VPO experiments.

The shape of the curves in Figures 6–9 suggest that the low-concentration extrapolation can give an estimate of the average size of an asphaltene monomer while the extrapolation at high concentration can, at best, give

Table 4. Estimated Monomer and Limiting Aggregate Molar Mass

solvent	temp. (°C)	molar mass (g/mol)	
		monomer	aggregate
C5-Asphaltenes			
toluene	50	1900	6200
	70	900	5000
1,2-dichlorobenzene	75	1500	4300
	130	2400	3600
C7-Asphaltenes			
toluene	50	400	10 000
	70	2500	8300
1,2-dichlorobenzene	75	900	6000
	130	3000	5300

an idea of the average limiting size of the asphaltene aggregates. The estimated monomer and aggregate molar masses of the Athabasca C5- and C7-asphaltenes for the different solvents and temperatures are summarized in Table 4. The estimated monomer molar mass is the infinitely dilute molar mass found by extrapolation of the molar masses measured at asphaltene concentrations from $<3 \text{ kg/m}^3$ to zero concentration, as shown in Figure 6. The estimated aggregate molar mass is the highest molar mass measured above 20 kg/m^3 asphaltene concentration.

On one hand, the apparent monomer molar mass appears to increase with temperature and shows no apparent relationship to solvent or asphaltene type. There is considerable scatter in the data and hence the relationship to temperature may be a coincidence. On the other hand, the limiting aggregate molar mass clearly depends on the solvent, temperature, and asphaltene type. The aggregate molar mass decreases as the temperature and the polarity of the solvent increase. The molar mass of the C7-asphaltenes is higher than that of the C5-asphaltenes. All of these trends are consistent with previous observations.^{16,17,27}

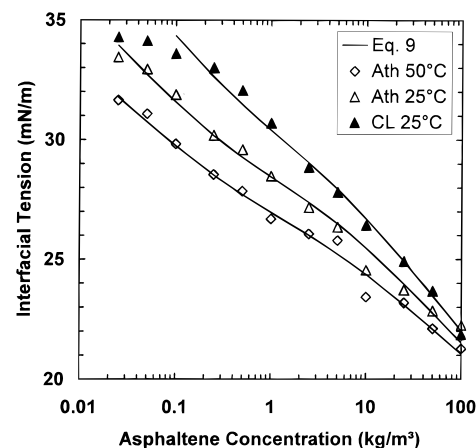
While the apparent changes in molar mass have not yet been verified with other techniques, there is some supporting evidence in the literature. Energy changes consistent with association have been observed over similar concentration ranges for other asphaltenes.²⁸ Furthermore, small-angle neutron and X-ray scattering techniques indicate that aggregates exist even at low concentrations. However, the molar masses measured here correspond to molecular dimensions that are smaller than the dimensions observed with small-angle neutron and X-ray scattering techniques. For example, a spherical aggregate with a molar mass of 6000 g/mol and a density of 1200 kg/m^3 has a radius of 1.3 nm compared to a radius of gyration from scattering measurements of 8 nm.²⁹ Part of the discrepancy may arise because the radius of gyration is expected to be larger than the physical radius. In addition, there is likely a lower resolution limit for the scattering measurements and the observed radius may be biased toward larger aggregates.

The results presented in Table 4 suggest that asphaltenes have an average monomer molar mass of 1800 g/mol and can associate into aggregates of 2–6 monomers, depending on the composition and temperature. If so, new approaches to modeling asphaltene precipitation may be required. For example, a small change in temperature or solvent composition may not affect the solubility of an asphaltene monomer. However, that small change may cause asphaltenes to aggregate and the much larger aggregates may be insoluble. Unless

Table 5. Fitting Parameters for Asphaltene Solvent versus Water Interfacial Tension

solvent	temp. (°C)	k (m^3/kg)	M_0 (g/mol)	M_e (g/mol)
C5-Asphaltenes				
toluene	50	0.380	1586	6407
	70	1.07	1000 ^a	5313
1,2-dichlorobenzene	75	0.771	1000 ^a	4480
	130	0.802	1801	3699
C7-Asphaltenes				
toluene	50	0.248	1000 ^a	10630
	70	0.146	2447	8750
1,2-dichlorobenzene	75	0.129	1000 ^a	6882
	130	0.254	2845	5238

^a M_0 fixed at 1000 g/mol if the initial curve gives values <1000 g/mol.

**Figure 10.** Interfacial tension of Athabasca (Ath) and Cold Lake (CL) C5-asphaltenes in toluene versus water.

the change in molar mass is accounted for, any solubility predictions are likely to be inaccurate. Both thermodynamic and colloidal approaches may need modification.

Curve Fits of Asphaltene Molar Mass. To interpret the interfacial tension data discussed later, equations relating asphaltene molar mass to concentration at different temperatures and in different solvents were required. Therefore, the VPO molar mass data were fitted with the following equation,

$$M_A = \frac{kC_A}{1 + kC_A}(M_e - M_0) + M_0 \quad (7)$$

where k , M_e , and M_0 are fit parameters. The value of M_0 corresponds to the average monomer molar mass and the value of M_e to the limiting average aggregate molar mass. The form of the curve fit was chosen because it provided a good fit, not because it is believed to represent the physics of the association. The fit parameters for the previously reported VPO data are given in Table 5 and the fitted equations are plotted in Figures 6–9.

Interfacial Tension Measurements. The apparent aggregation demonstrated in Figures 6–9 may be the result of reverse micellization. If so, a plot of interfacial tension of asphaltene–solvent mixtures versus water is expected to have the same form as Figure 3. Interfacial tensions versus water of Athabasca C5- and C7-asphaltenes in toluene are given in Figures 10 and 11, respectively, and those for Athabasca C5- and C7-asphaltenes in 1,2-dichlorobenzene are given in Figures 12 and 13, respectively. In all cases, the interfacial

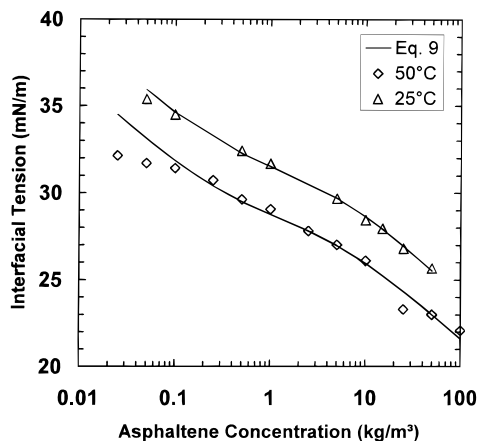


Figure 11. Interfacial tension of Athabasca C7-asphaltenes in toluene versus water.

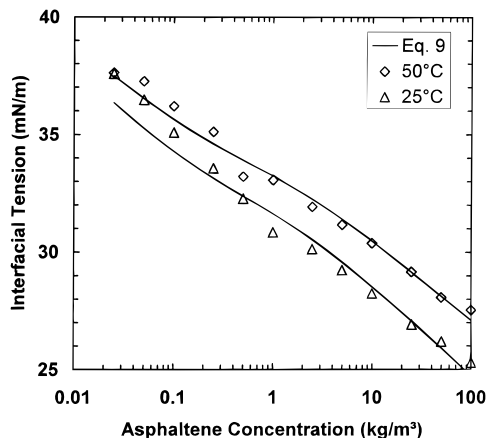


Figure 12. Interfacial tension of Athabasca C5-asphaltenes in 1,2-dichlorobenzene versus water.

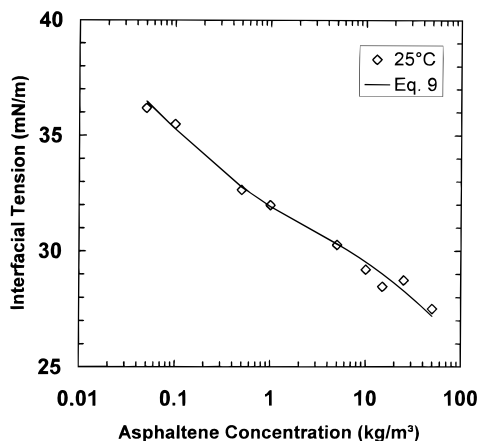


Figure 13. Interfacial tension of Athabasca C7-asphaltenes in 1,2-dichlorobenzene versus water.

tension decreases over the entire range of measured concentrations from 0.05 to 100 kg/m³. There is no evidence of a critical micelle concentration, although aggregation apparently occurs within the measured concentration range. Now, because asphaltenes are a multicomponent mixture rather than a pure surfactant, the formation of micelles and the appearance of a cmc may be complicated. Nonetheless, systems of mixed surfactants have been shown to form mixed micelles and to reach an invariant interfacial tension similar in appearance to a pure surfactant cmc.³⁰ Therefore, the monotonic decrease in interfacial tension with asphalt-

ene concentration indicates that the asphaltene aggregates are not reverse micelles.

Interestingly, the measured interfacial tensions appear to decrease linearly with an increase in log asphaltene concentration. Typically, this linear behavior would result from an increase in surfactant monomer concentration and yet, in this case, the surfactant monomers (the asphaltenes) are aggregating. To understand this behavior, it is necessary to review the thermodynamics of an interface. For an ideal mixture of pure surfactant in a solvent, the interfacial tension is related to surfactant concentration as follows,¹⁹

$$\frac{d\sigma}{d \ln(x_i)} = -RT\Gamma \quad (8)$$

where x_i is the equilibrium mole fraction of the surfactant. For dilute solutions, the mole fraction is directly related to the concentration,

$$x_i = \frac{C_i M_s}{\rho_s M_i} \quad (9)$$

where C_i is the surfactant concentration (kg/m³), M_i is the molar mass of the surfactant (g/mol), V_s is the volume of solvent (m³), ρ_s is the density of the solvent (kg/m³), and M_s is the molar mass of the solvent (g/mol). Usually, all of the variables except concentration are constant for a given surfactant–solvent mixture. Hence, $d \ln(x_i) = d \ln(C_i)$ and the expression for interfacial tension most commonly used in asphaltene research is found by straightforward substitution:

$$\frac{d\sigma}{d \ln(C_i)} = -RT\Gamma \quad (10)$$

However, if the surfactant aggregates, its molar mass varies and then $d \ln(x_i) = d \ln(C_i/M_i) = d \ln(C_i')$. The expression for interfacial tension is now given by

$$\frac{d\sigma}{d \ln(C_i')} = -RT\Gamma \quad (11)$$

where C_i' is the average molar concentration of the aggregating surfactant. It is implicitly assumed that the surface activity of the aggregate is approximately the same as that of a monomer. If we further assume that the surface coverage, Γ , of the aggregate is similar to that of a monomer, then a plot of interfacial tension versus the log of C_i' is expected to be linear.

The fitted molar mass data were used to calculate molar concentrations for all the interfacial tension data. For toluene at 50 °C, the fitted molar masses could be used directly because both VPO and interfacial tension data were collected at that temperature. For the remaining data, the values of k and M_0 determined at the closest temperature were used and a value of M_e was found by linear extrapolation with temperature. Once the fit equations were set, the slopes from eq 9 were found by linear regression. The slopes are given in Table 6 and the fitted interfacial tensions are shown in Figures 10–13. Note that the fits do not appear to be linear in Figures 10–13 because the interfacial tensions are plotted versus the asphaltene mass concentration rather than molar concentration.

The asphaltene surface coverages and interfacial areas per molecule, A , were calculated from the slopes

Table 6. Fitted Slopes from Eq 9 and Estimated Asphaltene Molecular Dimensions

solvent	temp. (°C)	slope (mN/m)	Γ (10^{-6} mol/m ³)	A (nm ²)	M_A (g/mol)
C5-Asphaltenes					
toluene	25	-1.85	0.75	2.2	1800
	50	-1.54	0.57	2.9	2670
1,2-dichlorobenzene	25	-1.72	0.70	2.4	1330
	50	-1.53	0.57	2.9	1640
C7-Asphaltenes					
toluene	25	-2.26	0.91	1.8	2000
	50	-2.14	0.80	2.1	2700
1,2-dichlorobenzene	25	-1.87	0.76	2.2	1770

of eq 9 and are given in Table 6. An estimate of molar mass can be made from the surface coverage if a molecular geometry is assumed. The asphaltene monomer molar masses are reported in Table 6; a spherical geometry on the interface and a density of 1200 kg/m³ are assumed. These values are rough estimates at best because (a) there may be up to 10% error in the measured slopes, (b) the aggregates may not have the same surface activity and surface coverage as the monomers, (c) the molecular geometry may not be spherical, and (d) the molecular geometry may vary with temperature and solvent. Nonetheless, the average estimated monomer molar mass of 1900 g/mol is within 100 g/mol of the monomer molar mass estimated from the VPO data.

Despite the approximations made in fitting the interfacial tension data, the results clearly indicate that the change in interfacial tension is consistent with a mixture of surface-active asphaltene monomers and aggregates. Reverse micelles can be ruled out for Athabasca asphaltenes in toluene and 1,2-dichlorobenzene. It seems likely that some other association mechanism applies in bitumens. The nature of that mechanism may be better explored by examination of the changes in chemical bonding in the concentration ranges over which association is observed.

Comparison with Cold Lake Asphaltenes. Preliminary molar mass and interfacial tension measurements were taken for Cold Lake C5-asphaltenes and are compared with the results for Athabasca C5-asphaltenes in Figures 6 and 10, respectively. The apparent molar mass of the Cold Lake asphaltenes follows the same trend as that of the Athabasca asphaltenes. The interfacial tension results indicate that the Cold Lake asphaltenes are somewhat less surface active (reduce interfacial tension less) than the Athabasca asphaltenes but again show no evidence of micelles. Hence, Cold Lake asphaltenes exhibit the same general behavior as Athabasca asphaltenes. The similarity suggests that it may be possible to apply the results from the Athabasca asphaltenes to other Western Canadian bitumen-derived asphaltenes.

The above results appear to contradict other reports in the literature of micelles in crude oils. However, in many cases, the literature evidence only indicates the formation of submicron particles (e.g., small-angle neutron or X-ray scattering studies⁸⁻¹¹) or of some form of association (e.g., calorimetry¹²). There is relatively little direct evidence of micelle formation from interfacial tension measurements,^{13,15} and there are other interfacial tension studies that show no evidence of micellization in crude oils.^{31,32} It is possible that micelles are a rare occurrence in crude oils. An investigation of oils from many sources is required to address the issue.

In any case, the different association behaviors likely arise from structural differences between asphaltenes from different sources because the elemental composition and functional group content appear to be similar for all asphaltenes.³³ For example, the shape of the molecule may prevent or enhance the potential for micellization.

Conclusions

The self-association of asphaltenes from Athabasca and Cold Lake bitumens was investigated in toluene at temperatures between 50 and 90 °C and 1,2-dichlorobenzene at temperatures between 75 and 130 °C. The association appeared to begin at concentrations below 0.5 kg/m³. Molar mass was constant at concentrations above 10–20 kg/m³ (1–2 wt %), suggesting that the aggregates reached a limiting size. The limiting aggregate molar mass decreases as the temperature and the polarity of the solvent increase. The limiting molar mass of the C7-asphaltenes is higher than that of the C5-asphaltenes. The average aggregate molar masses ranged from 4000 to 10 000 g/mol.

The molar mass of an asphaltene "monomer" from VPO and interfacial tension measurements is \approx 1800 g/mol. This molar mass is given by the intercept (at zero concentration) of a plot of measured molar mass versus asphaltene concentration. The plot can be linearly extrapolated to zero concentration only in the low-concentration region, that is, at asphaltene concentrations $<$ 3 kg/m³.

Asphaltene solubility is likely to depend strongly on the asphaltene molar mass. If asphaltene aggregation is as sensitive to solvent and temperature as these results suggest, then aggregation must be accounted for in asphaltene solubility models.

Both monomers and aggregates appear to be surface active. The change in interfacial tension upon asphaltene aggregation was fitted successfully when the change in asphaltene mole fraction upon aggregation was accounted for.

The aggregates that were observed in these experiments do not appear to be micelles. Interfacial tension did not stabilize at a constant value upon aggregation as would be expected with micelles. An investigation of the change in chemical bonding as the apparent association occurs may shed light on the association mechanism.

Acknowledgment

We are grateful to Imperial Oil Ltd. and the Natural Sciences and Engineering Research Council for financial support. We thank Ms. Olga Gafonova and Mr. Mayur Agrawala for completing the experimental work.

Nomenclature

- A = coefficient in VPO calibration equation
- C = mass concentration (kg/m³)
- C = molar concentration (mol/m³)
- d = diameter (m)
- ΔE = voltage difference (mV)
- g = gravitational acceleration (m/s²)
- k = molar mass fit parameter
- K = VPO calibration constant ((mV m³)/kmol)
- M = molar mass (g/mol)
- Q = flow rate (m³/s)
- R = universal gas constant (J/(mol K))

t = time
 T = temperature (K)
 V = volume (m³)
 x = mole fraction

Greek Symbols

Γ = surface coverage (mol/m²)
 σ = interfacial tension (N/m)
 ρ = density (kg/m³)

Subscripts

2 = solute
 A = asphaltene
 e = limiting aggregate
 eq = equilibrium
 i = surfactant
 o = monomer
 s = solvent

Literature Cited

- (1) Hirshberg, A.; deJong, N. J.; Schipper, B. A.; Meijer, J. G. Influence of Temperature and Pressure on Asphaltene Flocculation. *Soc. Pet. Eng. J.* **1984**, *24*, 283.
- (2) Pfeiffer, J. Ph.; Saal, R. N. Asphaltic Bitumen as Colloid System. *J. Phys. Chem.* **1940**, *44*, 139.
- (3) Dickie, J. P.; Yen, T. F. Macrostructures of the Asphaltic Fractions by Various Instrumental Methods. *Anal. Chem.* **1967**, *39*, 1847.
- (4) Storm, D. A.; Sheu, E. Y. Characterization of Colloidal Asphaltic Particles in Heavy Oil. *Fuel* **1995**, *74* (8), 1140.
- (5) Leonartis, K. J.; Mansoori, G. A. *Proceedings, SPE Symposium on Oilfield Chemistry*, Richardson, TX, 1987; Society of Petroleum Engineers: Dallas, TX, 1987; SPE Paper 16258.
- (6) Andersen, S. I. Hystersis in Precipitation and Dissolution of Petroleum Asphaltenes. *Fuel Sci. Technol. Int.* **1992**, *10* (10), 1743.
- (7) Singh, C.; Peramanu, S.; Yarranton, H. Experimental Study on the Reversibility of Asphaltene Precipitation. Student Paper, Presented at the 49th Canadian Chemical Engineering Conference, Saskatoon, Oct 3–6, 1999.
- (8) Ravey, J. C.; Ducouret, G.; Espinat, D. Asphaltene Macrostructure by Small Angle Neutron Scattering. *Fuel* **1988**, *67*, 1560.
- (9) Sheu, E. Y.; Storm, D. A.; De Tar, M. M. Asphaltenes in Polar Solvents. *J. Non-Cryst. Solids* **1991**, *131–133*, 341.
- (10) Carnahan, N. F.; Quintero, L.; Pfund, D. M.; Fulton, J. L.; Smith, R. D.; Capel, M.; Leontaritis, K. A Small-Angle X-ray Scattering Study of the Effect of Pressure on the Aggregation of Asphaltene Fractions in Petroleum Fluids under Near-Critical Solvent Conditions. *Langmuir* **1993**, *9*, 2035.
- (11) Xu, Y.; Koga, Y.; Strausz, O. P. Characterization of Athabasca Asphaltenes by Small-Angle X-ray Scattering. *Fuel* **1995**, *74* (7), 960.
- (12) Andersen, S. I.; Christensen, S. D. The Critical Micelle Concentration of Asphaltenes as Measured by Calorimetry. Proceedings of the AIChE National Spring Meeting, March 14–18, 1999; p 16.
- (13) Sheu, E. Y.; Storm, D. A. In *Asphaltenes Fundamentals and Applications*; Sheu, E. Y., Mullins, O. C., Eds.; Plenum Press: New York, 1995; p 1.
- (14) Rogocheva, O. V.; Rimaev, R. N.; Gubaidullen, V. Z.; Khakimov, D. K. Investigation of the Surface Activity of Petroleum Residues. Translated from *Kolloid. Zh.* **1980**, *42* (3), 586.
- (15) Mohamed, R. S.; Ramos, A. C. S.; Loh, W. Aggregation Behavior of Two Asphaltic Fractions in Aromatic Solvents. *Energy Fuels* **1999**, *13*, 323.
- (16) Moschopedis, S. E.; Fryer, J. F.; Speight, J. G. Investigation of Asphaltene Molecular Weights. *Fuel* **1976**, *55*, 227.
- (17) Wiehe, I. A. A Solvent-Resid Phase Diagram for Tracking Resid Conversion. *Ind. Eng. Chem. Res.* **1992**, *31* (2), 530.
- (18) Peramanu, S.; Pruden, B. P.; Rahimi, P. Molecular Weight and Specific Gravity Distributions for Athabasca and Cold Lake Bitumens and Their Saturate, Aromatic, Resin and Asphaltene Fractions. *Ind. Eng. Chem. Res.* **1999**, *38* (8), 3121.
- (19) Yarranton, H. W.; Masliyah, J. H. Molar Mass Distribution and Solubility Modeling of Asphaltenes. *AIChE J.* **1996**, *42*, 3533.
- (20) Yan, Z.; Elliot, J. A. W.; Masliyah, J. H. Roles of Various Bitumen Components in the Stability of Water-in-Diluted-Bitumen Emulsions. *J. Colloid Interface Sci.* **1999**, *220*, 329.
- (21) Chung, K. E.; Anderson, L. L.; Wiser, W. H. New Procedure for Molecular Weight Determination by Vapor Pressure Osmometry. *Fuel* **1999**, *58*, 847.
- (22) Li, B.; Fu, J. Interfacial Tension of Two-Liquid-Phase Ternary Systems. *J. Chem. Eng. Data* **1992**, *37*, 172.
- (23) Campanelli, J. R.; Wang, X. Effect of Neck Formation on the Measurement of Dynamic Interfacial Tension in a Drop Volume Tensiometer, Note. *J. Colloid Interface Sci.* **1997**, *190*, 491.
- (24) Campanelli, J. R.; Wang, X. Comments on the Modelling the Diffusion Controlled Adsorption of Surfactants. *Can. J. Chem. Eng.* **1998**, *76*, 51.
- (25) Joos, P.; Fang, J. P.; Serrien, G. Comments on Some Dynamic Surface Tension Methods by the Dynamic Bubble Pressure Method. *J. Colloid Interface Sci.* **1992**, *151*, 144.
- (26) Hiemenz, P. C.; Rajapopalan, R. *Principles of Colloid and Surface Chemistry*, 3rd ed.; Marcel Dekker Inc.: New York, 1997; p 360.
- (27) Andersen, S. I. Dissolution of Solid Boscan Asphaltenes in Mixed Solvents. *Fuel Sci. Technol. Int.* **1994**, *12* (11&12), 1551.
- (28) Andersen, S. I.; Birdi, K. S. Aggregation of Asphaltenes as Determined by Calorimetry. *J. Colloid Interface Sci.* **1991**, *142* (2), 497.
- (29) Sirota, E. B. Swelling of Asphaltenes. *Pet. Sci. Technol.* **1998**, *16*, 415.
- (30) Mulqueen, M.; Blankschtein, D. Prediction of Equilibrium Surface Tension and Surface Adsorption of Aqueous Surfactant Mixtures Containing Ionic Surfactants. *Langmuir* **1999**, *15*, 8832.
- (31) Sheu, E. Y.; De Tar, M. M.; Storm, D. A. Interfacial Properties of Asphaltenes. *Fuel* **1992**, *71*, 1277.
- (32) Acevedo, S.; Escobar, G.; Ranaudo, M. A.; Khazen, J.; Borges, B.; Pereira, J. C.; Mendez, B. Isolation and Characterization of Low and High Molecular Weight Acidic Compounds from Cerro Negro Extraheavy Crude Oil. *Energy Fuels* **1999**, *12*, 333.
- (33) Speight, J. G. *The Chemistry and Technology of Petroleum*, 3rd ed.; Marcel Dekker: New York, 1999; pp 419–436.

Received for review January 19, 2000

Revised manuscript received April 17, 2000

Accepted May 1, 2000

IE000073R